# Tech Note: Application of ImPASS processing to images captured for Fourier Ptychography and Structured Illumination Microscopy

James N. Caron
Research Support Instruments, 4325-B Forbes Boulevard, Lanham, MD 20706, USA
Quarktet, 205 Indian Spring Drive, Silver Spring, MD 20901, USA
Caron@RSImd.com

September 6, 2023

## Abstract

Image Phase Alignment Super-sampling (ImPASS), Fourier Ptychography, and Structured Illumination Microscopy are computational imaging methods that combine a series of low-resolution images into a single high-resolution image. All three methods process the image sets in the Fourier domain. There has been speculation on whether ImPASS is related to one of the other methods. To gain insight on this question, ImPASS processing was applied to image sets created for the other methods to assess similarities between the methods.

## 1 Introduction

Image Phase Alignment Super-sampling (ImPASS) is a computational imaging method that combines a sequence of slightly-displaced low-resolution images to create a single high-resolution image. The approach was first presented in 2004 [1] but recent work demonstrated that the process can yield super-resolution in addition to super-sampling. [2] Super-resolution is defined here as image resolution that exceeds the diffraction limit of the optical system. The image acquisition is comparatively simple, requiring no specialized optics or active illumination of the target. Either the camera or scene is translated by fractions of a pixel to produce the slightly displaced image set. Processing consists of image registration, interpolation, and application of blind deconvolution. [3]

ImPASS has been compared to the Fourier Ptychography and Structured Illumination. Fourier Ptychography (FP) also produces a single high-resolution image from a set of comparatively low-resolution images. The sample is illuminated by an LED array where individual LEDs can be selectively activated. [5, 4] This allows capture of a sequence where each frame is illuminated from a different angle. FP processing typically consists of applying an iterative phase retrieval process in the Fourier domain to reconstruct the high resolution image. [6] For Structured Illumination Microscopy (SIM), [7] low-resolution images are acquired as the sample is illuminated with a sinusoidal-like pattern. This pattern is displaced or rotated for every new image to build a sequence. The images are processed using a phase optimisation method or similar technique [8, 9] to create a single image with higher resolution.

All three methods make use of processing in the Fourier domain to reconstruct high resolution information. It is important to note that the term 'phase' is used differently for these methods. For FP and SIM, 'phase' refers to the phase of the electromagnetic wave incident on the sample. For ImPASS, phase refers to the phase component of the Fourier transform of an image.

A question posed by reviewers was whether ImPASS is a distinct approach or a variation of either FP or SIM techniques. ImPASS is not mature enough for this to be determined through theory. Alternatively, insight can be gained by applying ImPASS image processing to image sets created for these other methods. If application of ImPASS processing produces significant super-sampling or super-resolution, then the information gathered from these methods is related. Further investigation of the technique's similarities

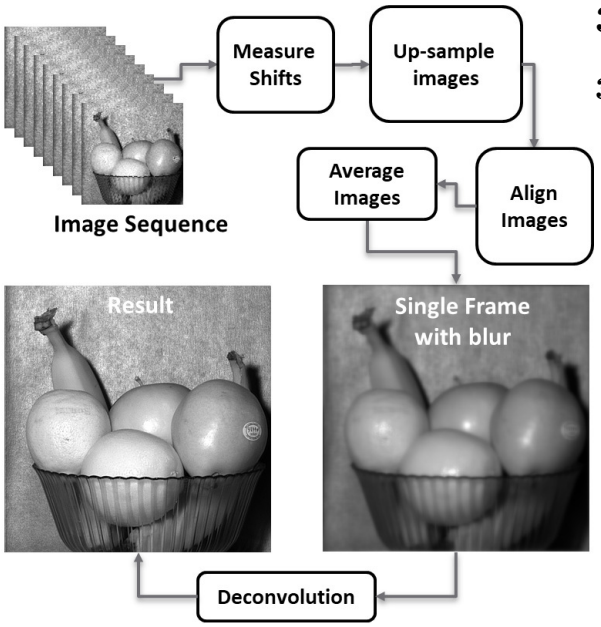


Figure 1: Processing flow chart for ImPASS. Slightly-displaced low-resolution images are aligned, up-sampled and averaged. Blind deconvolution is applied to produce a single high-resolution image. (Picture Credit: Author)

would be warranted. However, if the results of this exercise are not positive, this supports the argument that ImPASS is distinct from FP or SIM.

# 2 ImPASS Image Processing

A full description of the ImPASS processing approach was provided in Reference [3] but is summarized here. The processing flow, shown in Figure 1, consists of four primary steps. Unless image displacements are determined by some other means, phase correlation [10] is used to determine translation differences between each frame and a reference image. Corrective alignments are applied to the images after up-sampling to the images. The up-sampled images are averaged together to produce a single image with resolution consistent with the low-resolution images. [2] Application of the blind deconvolution method SeDDaRA [11] produces the super-sampled information.

# 3 Processing Results

## 3.1 FP Image Set

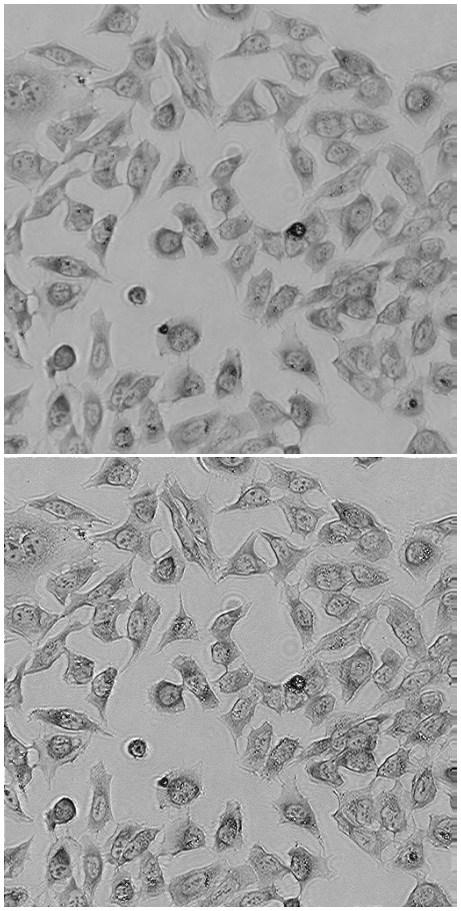

Figure 2: (Top) A single frame of the "stained" image set showing fixed human osteosarcoma epithelial cells. (Bottom) Application of SeDDaRA to a single image produces significant resolution improvements as a result of optical blur removal. (Picture Credit: University of California, Berkeley, open domain)

The FP image sets used for this study were created and provided by the Computational Imaging group at University of California, Berkeley, and are available as open source. [12, 13] ImPASS was applied to seven sets with no significant differences in the results, regardless of target. The representative set displayed in Figure 2 originally consisted of 202 images of fixed human osteosarcoma epithelial (U2OS) cells with image dimensions 2560 X 2160 pixels. Processing with FP improved the resolution from numerical aperture of 0.2 to 0.7. [13] Most frames in this set were

considered 'dark field' where illumination of the sample originated from outside the optics' field-of-view. Initial attempts at ImPASS processing showed that inclusion of dark field images produced adverse artifacts in the processed result. As such, processing was limited to the 20 suitable light field images, those in which the illumination was within the field of view. The images were cropped to size $512^2$ pixels (shorthand for $512 \times 512$).

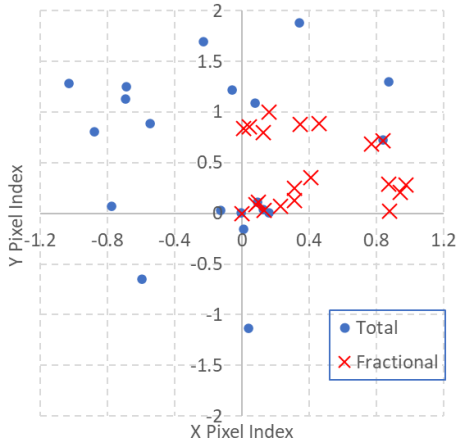


Figure 3: The frame-by-frame displacements (circles) of the "stained" set in pixels as determined by phase correlation. The fractional portion of the displacements (crosses) reveal that there are large gaps in the pixel space.

Application of phase correlation to this set produced frame displacements as a function of pixel index, as shown in Figure 3. The goal for effective ImPASS processing is to evenly sample the pixel space. At first glance, this data seems to be somewhat evenly spaced, but integer movements do not contribute additional information to the set. For example, a shift of 1.2 does not add any information that is not provided by a shift of 0.2 or -0.8. When the integer shifts are removed, as shown in Figure 3(crosses), considerable gaps in the pixel space are evident. This limits the resolution that can be recovered.

An additional issue with this set is that while the images can be aligned globally, the features, being three dimensional cells being illuminated from different angles, do not align locally. ImPASS has only previously been applied to image sets that possess spatially invariant displacements.

The final step is application of blind deconvolution. This process not only recovers the super-sampled resolution but also removes optical blur. As such it is important to compare the blind deconvolution of low-resolution images to blind deconvolution of the up-sampled combined images to ensure that resolution improvement can be attributed to super-sampling. The deconvolution of a single frame, shown in Figure 2(bottom), demonstrates that there is considerable optical blur in this image set.

The aligned image set was up-sampled in steps by a factor of $M_{SS} = 8$ creating images of size $4096^2$ pixels. The central $1024^2$ pixel portion of the image is shown in Figure 4 (top) alongside a representative deconvolution. The result has some artifacts in the form of vertical bars that can be attributed to insufficient pixel sampling, but there is a visible improvement in resolution. This improvement, however, is not significantly greater than that achieved by applying deconvolution to the original image.

This was also the case for the other six FP images sets. Application of ImPASS to FP-created images sets did not result in super-sampled images, i.e. resolution that is smaller than the pixel size of sensor.

## 3.2 SIM Image Set

Six SIM data sets were acquired from the University of Bielefeld Biophotonics Group github site. [14] The images were provided as open-source for reference [15] and development of the fairSIM method. The sets varied in number of frames and image sizes. ImPASS was applied to all six sets with generally the same results. The representative set, referred to as 'OMX-U2OS-Tubulin-525nm', had 120 frames with image size of $512^2$ pixels and description 'U2OS, Tubulin stain excitation at 488nm, emission at approx. 525nm'. Forty frames were removed as the images had significant blur, leaving 80 frames for the processing.

Application of phase correlation image registration to the SIM set produced shifts that were close to zero. The data is shown in Figure 5 where the dotted circle represents the accuracy of the registration. [16] This suggests that SIM frames do not have significant displacements and the pixel space is not sufficiently sampled. ImPASS processing was applied to both aligned and non-aligned sets with no significant difference in the results. A portion of the average of the low resolution set (top) and the subsequent blind de-

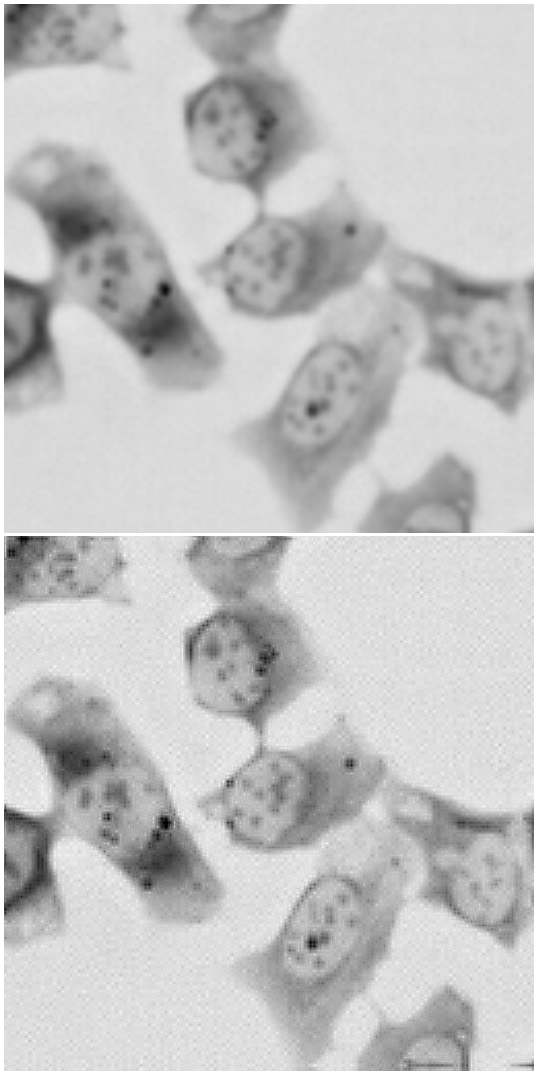

Figure 4: A portion of the SIM up-sampled, combined image before (top) and after (bottom) deconvolution. The improvement in resolution is not sufficient to attribute to super-sampling.

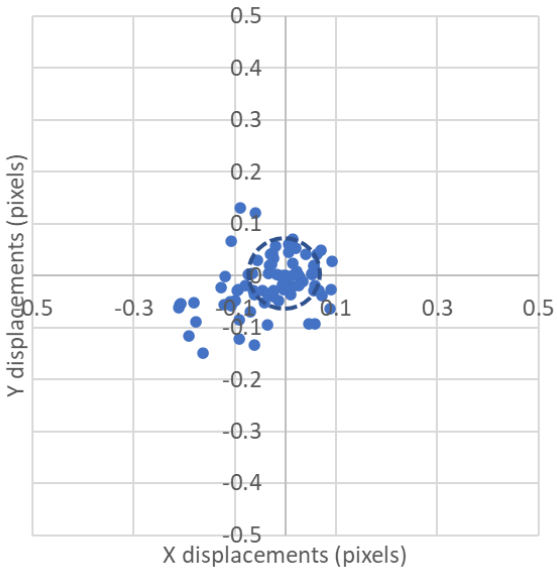


Figure 5: Frame displacement measurements of the OMX-U2OS data set. Most measurements fall within 1/17 of a pixel, the measured accuracy of the alignment.

convolution (bottom) is shown in Figure 6. The deconvolution is slightly clearer indicating that the image set contains some optical blur.

Figure 7 shows a portion of the up-sampled ($M_{SS} = 8$) image on the top and the ImPASS result on the bottom. The final image is somewhat clearer but resolves no features that are not visible in the low-resolution deconvolution (Figure 7 (bottom)). This image can be directly compared to the result of SIM processing in Reference [15] supplemental Figure 3d which achieves greater resolution. The arrow points to a feature that was resolved as two strands using SIM but is not resolved by ImPASS.

# 4 Comments

ImPASS processing was applied to image sets created for comparable technologies to assess the relation between the methods. Seven sets of FP images were processed where ImPASS produced no significant super-sampling. Six sets of SIM images were processed using the ImPASS algorithm, also without any evidence of super-sampling. As such, information obtained using FP or SIM is distinct from information obtained by collecting slightly displaced images. This provides evidence than ImPASS can be considered a distinct tech-

nology from these other methods.

Funding This work was funded using the RSI internal resources and the author's personal time.

Disclosures The author has no conflicts to disclose.

Data Availability Statement The data that support the findings of this study are available from the corresponding author upon reasonable request.

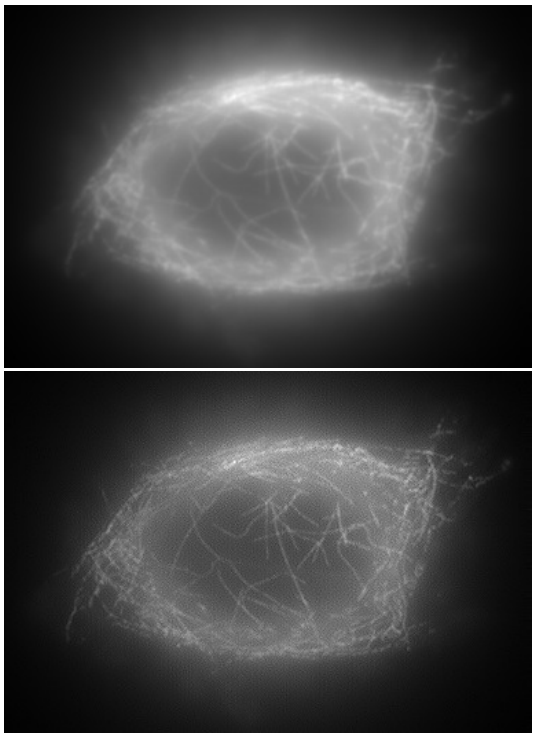

Figure 6: (Top) The average of 80 frames from the "OMX-U2OS-Tubulin-525nm" set at the original resolution without alignment. (Bottom) Application of SeDDaRA blind deconvolution removes some optical blur from the image. (Image Credit: University of Bielefeld Biophotonics group, open source)

# References

[1] J. N. Caron, "Rapid supersampling of multiframe sequences by use of blind deconvolution," Opt. lett. **29**(17), 1986-1988, (2004).

[2] J. N. Caron, "Application of ImPASS to translated images produces image resolution below the optical diffraction resolution limit," AIP Adv. **12**(4), 045305, (2022).

[3] J. N. Caron, "Utilization of image phase information to achieve super-sampling," Appl. Opt. **59**(23), 7066-7073 (2020).

[4] P. Chandra Konda, L. Loetgering, K. C. Zhou, S. Xu, A. R. Harvey, and R. Horstmeyer, "Fourier ptychography: current applications and future promises," Opt. Express **28**, 9603-9630 (2020).

[5] G. Zheng, C. Shen, S. Jiang, P. Song, and C. Yang, "Concept, implementations and applications of Fourier ptychography," Nat. Rev. Phys **3**(3), 207-223 (2021).

[6] L-H Yeh, J. Dong, J. Zhong, L. Tian, M. Chen, G. Tang, M. Soltanolkotabi, and L. Waller, "Experimental robustness of Fourier ptychography phase retrieval algorithms." Opt. Express **23**(26), 33214-33240 (2015).

[7] M. Saxena, G. Eluru, and S. Siva Gorthi, "Structured illumination microscopy," Adv. Opt. Photonics **7**(2), 241-275 (2015).

[8] K. Wicker, O. Mandula, G. Best, R. Fiolka, and R. Heintzmann, "Phase optimisation for structured illumination microscopy," Opt. Express **21**, 2032–2049 (2013).

[9] A. Lal, C. Shan, and P. Xi, "Structured illumination microscopy image reconstruction algorithm," IEEE J. Sel. Top. Quantum Electron **22**(4), 50-63 (2016).

[10] X. Tong, Z. Ye, Y. Xu, S. Gao, H. Xie, Q. Du, S. Liu, X. Xu, S. Liu, K. Luan, and U. Stilla, "Image registration with Fourier-based image correlation: A comprehensive review of developments and applications," IEEE J. Sel. Top. Appl. Earth Obs. Remote Sens. **12**(10), 4062-4081 (2019).

[11] J. N. Caron, N. M. Namazi, and C. J. Rollins, "Noniterative blind data restoration by use of an extracted filter function," Appl. Opt. **41**(32), 6884-6889, (2002).

[12] R. Eckert, Z. F. Phillips, and L. Waller, "Efficient illumination angle self-calibration in Fourier ptychography," Appl. Opt. **57**, 5434-5442 (2018).

[13] L. Tian, Z. Liu, L-H Yeh, M. Chen, J. Zhong, and L. Waller, "Computational illumination for high-speed in vitro Fourier ptychographic microscopy," Optica **2**(10), 904-911 (2015).

[14] M. Müller, "fairSIM/fairSIM Documentation," GitHub Repository (2018).

[15] M. Müller, V. Mönkemöller, S. Hennig, W. Hübner, and T. Huser, "Open-source image reconstruction of super-resolution structured illumination microscopy data in ImageJ," Nat. Commun. **7**(1), 1-6 (2016).

[16] J.N. Caron, M. J. Montes, and J. L. Obermark, "Extracting flat-field images from scene-based image sequences using phase correlation," Rev. Sci. Instrum. **87**(6), 063710 (2016).

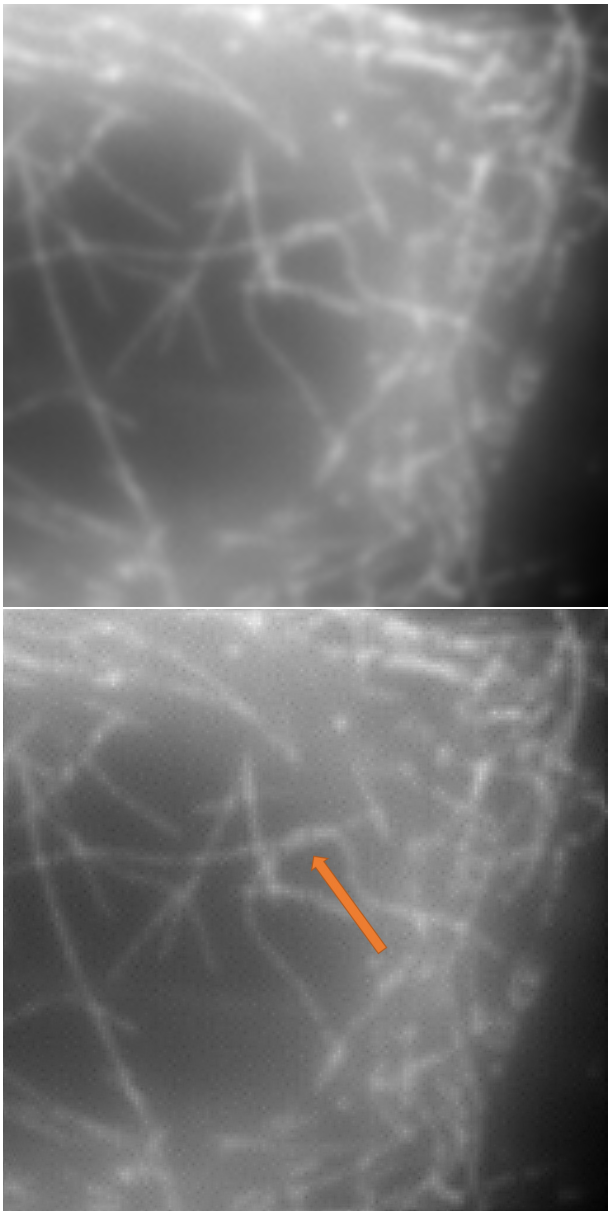

Figure 7: (Top) A $76^2$ pixel region of the upsampled, combined image before deconvolution is applied. (Bottom) The image after deconvolution. The arrow points to two strands that are resolved using SIM processing not resolved by the ImPASS process.